

**Table 1** Details of primary antibodies used

Primary Antibody	Source	Isotype	Antigen retrieval methods	Concentration ( $\mu\text{g/mL}$ )
PICP (Millipore Corporation, Beillerica, MA)	Rat	IgG <sub>1</sub>	AC	0.03
Type I collagen (Abcam, Cambridge, UK)	Mice	IgG <sub>1</sub>	AC	$\times 600^a$
ICTP (from Dr Risteli)	rabbit	polyclonal	MW	0.1
MMP-2 (Millipore Corporation)	Rabbit	Polyclonal	none	1.7
TIMP-2 (Millipore Corporation)	Rabbit	polyclonal	none	10
$\alpha$ -smooth muscle actin (Dako Japan, Tokyo, Japan)	Mice	IgG <sub>2a</sub> $\kappa$	none	$\times 100^a$
CD34 (Nichirei, Tokyo, Japan)	Mice	IgG <sub>1</sub>	MW	0.1
D2-40 (Nichirei)	Mice	IgG <sub>1</sub>	MW	0.26

MW, microwave irradiation for 2 minutes at 1000 W in the citrate buffer (pH 6.0); AC, autoclave for 5 minutes at 121°C.

<sup>a</sup> Indicates the dilution.

saline, they were incubated overnight with primary antibodies at 4°C. The antigen-antibody reaction was visualized by 3,3'-diaminobenzidine tetrahydrochloride. The sections were counterstained using resorcin-fuchsin and hematoxylin. As a reference for background staining, murine isotype-matched, nonspecific monoclonal IgG1 or normal rabbit serum was used.

Dual immunohistochemical staining using CD34 and D2-40 was performed as described previously [31]. Antigen-antibody reactions were visualized by using Vector Red (Vector Laboratories, Burlingame, CA) and diaminobenzidine tetrahydrochloride.

### 2.3. Morphometry analyses

The area densities of the Al-B<sup>+</sup> stain and the ICTP<sup>+</sup> expression contained in FF, namely,  $A_A(\text{Al-B})$  and  $A_A(\text{ICTP})$ , and the number density of the CD34<sup>+</sup> capillary, namely,  $N_A(\text{cap})$ , were estimated in relation to FF from each section [36].

To quantitatively estimate the change in ECM remodeling in FF, we used volume density:  $V_V(\text{Al-B})$ , which is the total volume of the Al-B<sup>+</sup> stain in a unit volume.  $V_V(\text{Al-B})$  was estimated with the aid of a basic principle of stereology [36]:

$$V_V(\text{Al-B}) = A_A(\text{Al-B}) \quad (1)$$

Here,  $A_A(\text{Al-B})$  is area density defined as the fraction of the Al-B<sup>+</sup> staining area contained in the whole area of a fibroblastic focus. Moreover,  $A_A(\text{ICTP})$  was also estimated. The sections stained by Al-B or immunostained by the antibody against ICTP were magnified by a charged coupled device (CCD) camera (Motic Images Plus 2.0S image analysis system; Shimazu, Kyoto, Japan), and the profiles were measured by adopting the point-counting method using a grid of 2- $\mu\text{m}$  of intervals.

The degree to which capillaries developed in the lung tissue was quantified in terms of their length density in space:  $L_V(\text{cap})$ , which is the total length of the capillaries in a unit volume. This was estimated by resorting to a basic principle of stereology [36]:

$$L_V(\text{cap}) = 2N_A(\text{cap}) \quad (2)$$

Here,  $N_A(\text{cap})$  is the numerical density of capillaries in terms of area or the number of capillaries in a unit area. In the present study,  $N_A(\text{cap})$  was estimated as the number density of capillaries in 100- $\mu\text{m}^2$  area of a fibroblastic focus. The area of FF was measured using a digitizer, and the number of capillaries contained in FF was counted using an ocular microscope.

### 2.4. Statistical analysis

The relationship between the area densities of Al-B<sup>+</sup> and ICTP<sup>+</sup> and the relationship between the area density of ICTP and the capillary number density were evaluated using the Spearman rank correlation coefficient. A *P* value of less than .05 was considered as statistically significant.

## 3. Results

### 3.1. Characterization of FF by Alcian blue staining and immunostaining with carboxyterminal telopeptide of type I collagen

We characterized FF with Al-B staining and immunostaining using primary antibodies against PICP, type I collagen, and ICTP. The FF were characterized as having 3 patterns. The first set of serial sections showed an Al-B-dominant pattern. The whole ECM of a fibroblastic focus was strongly stained with Al-B (Fig. 1A), whereas immunostaining revealed low expression levels of type I collagen and ICTP (Fig. 1B, C). The expression of PICP was found to be consistent in fibroblasts of the focus (Fig. 1D). The second set of serial sections showed a mixed pattern of Al-B staining and collagen markers: Al-B stained the inner side of a fibroblastic focus, whereas the expression of type I collagen, and ICTP was noted in the peripheral regions where Al-B staining was not detected (Fig. 2A-C). The third set of serial sections showed a collagen-dominant pattern. The expression of type I collagen and ICTP was detected in the whole ECM of a fibroblastic focus, whereas weak staining was observed with Al-B (Fig. 3A-C). FF

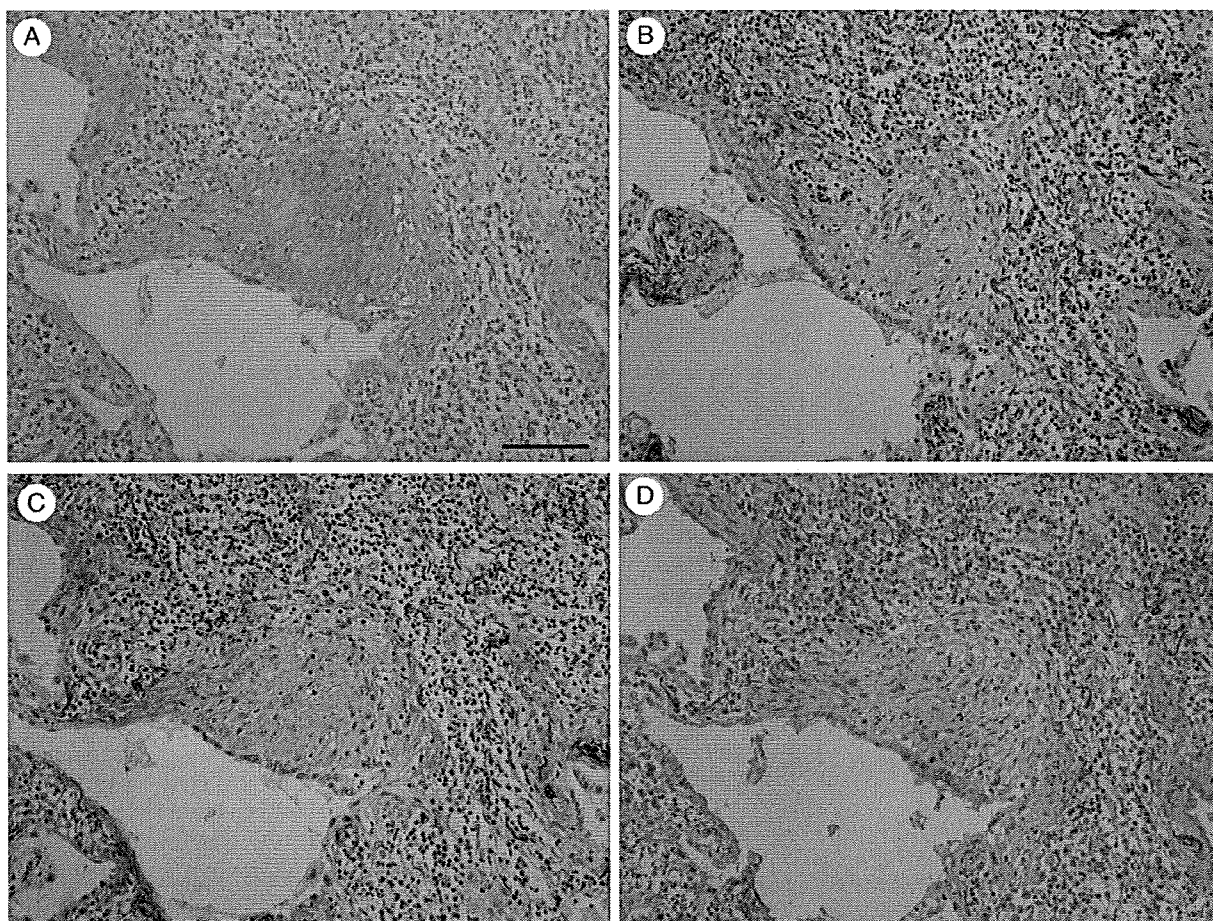


**Fig. 1** An Al-B–dominant pattern of fibroblastic foci. The first set of serial sections shows that Al-B strongly stains in the whole ECM of a fibroblastic focus (A), whereas the expression of type I collagen (B) and ICTP (C) is barely observed in the focus. D, The expression of PICP is observed in fibroblasts of the focus. Hematoxylin (A–D) and Resorcin-fuchsin (B–D) for counterstain. Scale bar represents 100  $\mu\text{m}$ .

exhibiting this pattern typically had a low expression of PICP in the fibroblasts, although high PICP expression was occasionally observed (Fig. 3D). The distribution of ICTP expression was found to be similar to that of mature type I collagen for all 3 staining patterns. Compared with immunostaining with antibodies against type I collagen, immunostaining with antibodies against ICTP showed less architectural deviation with regard to antigen retrieval; therefore, in the present study, we used ICTP as the marker for deposition of type I collagen. No specific trend was observed in any of the 3 aforementioned patterns with respect to the expression of  $\alpha$ -smooth muscle actin in the fibroblasts (data not shown).

### 3.2. A negative correlation between Al-B+ and ICTP+ area densities in FF and the staging of FF

The area densities of Al-B<sup>+</sup> and ICTP<sup>+</sup> in FF were measured. The results demonstrated that a significantly negative correlation existed between  $A_A(\text{Al-B})$  and  $A_A(\text{ICTP})$

( $r = -0.832, P < .001$ ) (Fig. 4). It has been previously reported that the deposition of PGs in FF occurs before the deposition of collagen [30]. Therefore, the 3 patterns observed on Al-B staining and immunostaining were defined as 3 stages: stage I [ $A_A(\text{Al-B}) > 75\%$ ], stage II [ $75\% > A_A(\text{Al-B}) > 25\%$ ], and stage III [ $A_A(\text{Al-B}) < 25\%$ ]. Stage II was observed in all 16 patients. Stages I and III were not identified in 2 and 3 patients, respectively (Table 2).

### 3.3. Stage-specific characterization of MMP-2 and TIMP-2 expression

The distribution of MMP-2 and TIMP-2 expression was characterized for each stage. In stage I, both MMP-2 and TIMP-2 were expressed in the fibroblasts and the overlying epithelium (Fig. 5A–C). In the later stages, the expression of TIMP-2 was attenuated both in the fibroblasts and the overlying epithelium. In contrast, the expression of MMP-2 persisted in the fibroblasts, although it was not observed in the overlying epithelium (Fig. 5D–F).

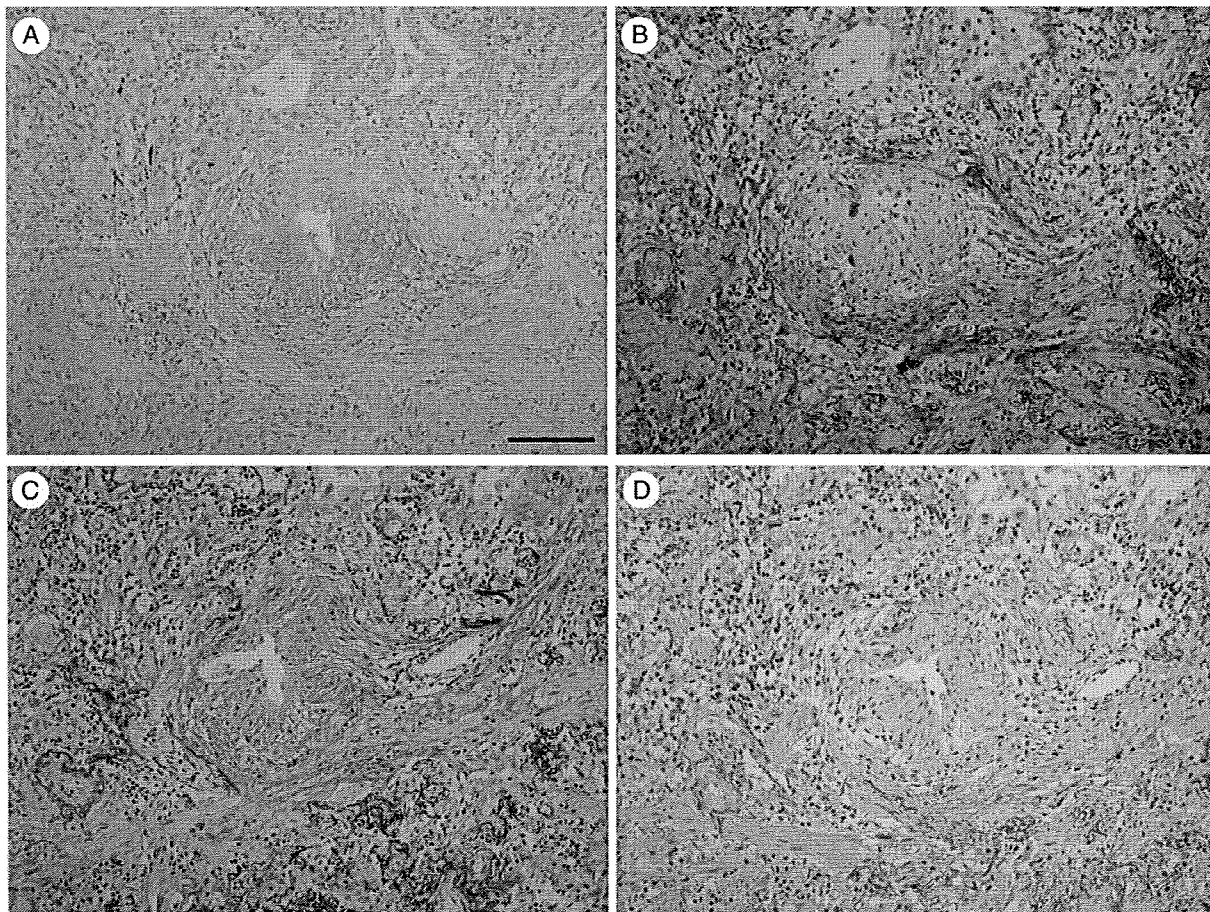


**Fig. 2** A mixed pattern of fibroblastic foci. The second set of serial sections shows that Al-B stains in the inner side of a fibroblastic focus (A), whereas the expression of type I collagen (B) and ICTP (C) is observed in the peripheral side where Al-B staining is not detected. D, The expression of PICP is only observed in the inner side of fibroblasts in the focus. Hematoxylin (A-D) and Resorcin-fuchsin (B-D) for counterstain. Scale bar represents 100  $\mu\text{m}$ .

### 3.4. Stage-specific characterization of capillary angiogenesis and lymphangiogenesis

The distribution of blood and lymphatic vessels in the 3 stages was investigated.  $\text{CD34}^+$  capillaries were absent in stage I (Fig. 6A, B); a small number of capillaries were observed in the  $\text{ICTP}^+$  lesions in stage II (Fig. 6C, D); and the capillaries were found to be widely distributed in stage III (Fig. 6E, F). Morphometric analysis demonstrated that a significant correlation exists between  $A_A(\text{ICTP})$  and  $N_A(\text{cap})$  ( $r = 0.488$ ,  $P < .001$ ) (Fig. 6G). On the other hand,  $\text{D2-40}^+$  lymphatic vessels were undetectable in the FF across all 3 stages (Fig. 6B, D, F).

## 4. Discussion

In the present study, 3 different patterns of Al-B staining and ICTP immunostaining was observed in FF—Al-B-dominant, ICTP-dominant, and mixed. The results obtained

indicate that the deposition of GAGs and collagen in FF may be regulated via 2 distinct processes. Bensadoun et al [30] have reported that the deposition of  $\text{Al-B}^+$  GAGs in lesions associated with IPF, bronchiolitis obliterans organizing pneumonia, and diffuse alveolar damage (DAD) is dependant on the deposition of versican, which is a type of PG. Although collagen deposition was barely detected in lesions with versican deposition, type I procollagen was expressed in the myofibroblasts present in the lesions; thus, they hypothesized that this PG may influence early repair processes in IPF before collagen deposition. Our findings were consistent with those of Bensadoun et al. Moreover, a morphological analysis of the mixed pattern demonstrated that collagen deposition was dominant in the region outside the FF where GAG degradation was observed. A significant negative correlation was observed between the  $\text{Al-B}^+$  and  $\text{ICTP}^+$  area densities in the FF. These results suggest that the deposition of collagen begins after the degradation of GAGs. Based on these histopathologic characteristics, 3 stages were defined in FF, namely, stage I, characterized by GAG-dominant deposition; stage II, characterized by mixed

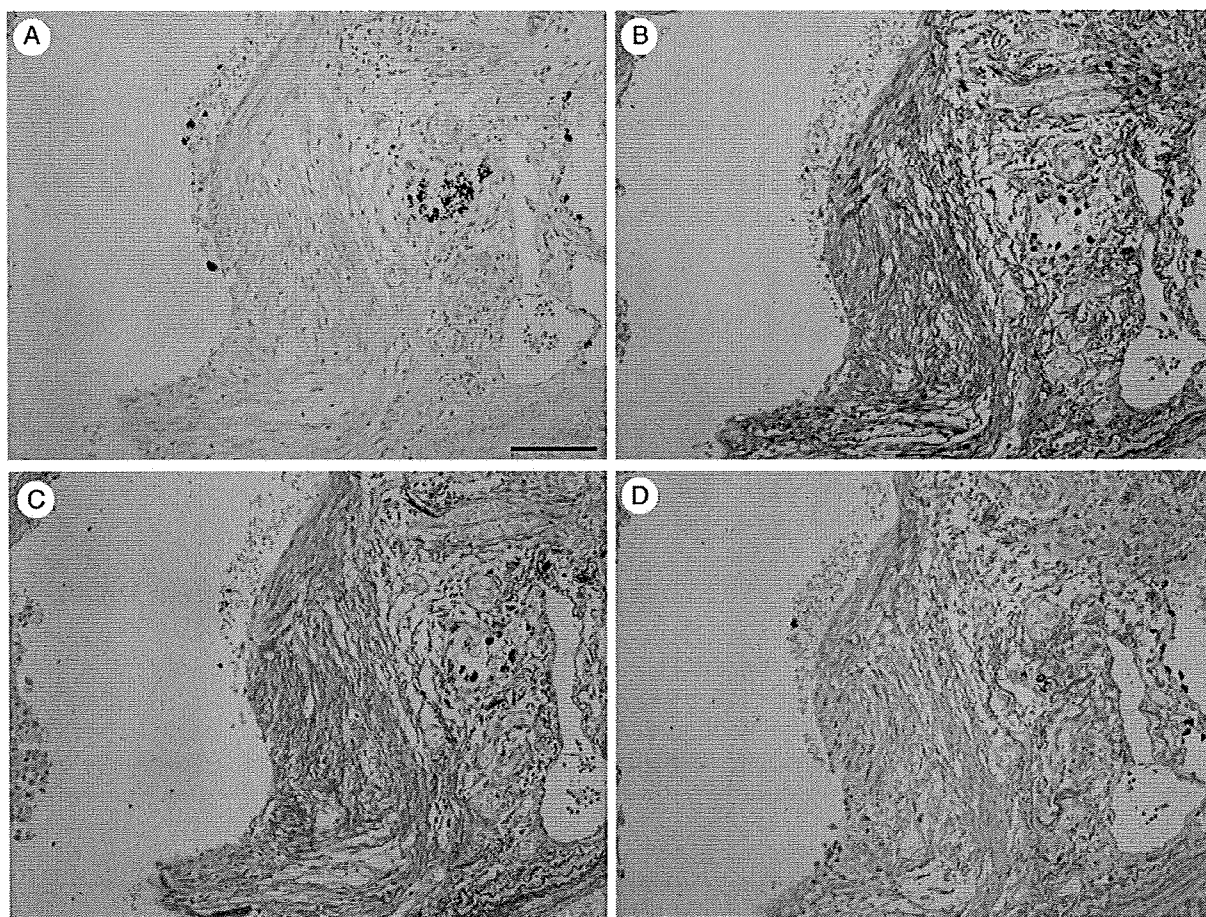


**Fig. 3** A collagen-dominant pattern of fibroblastic foci. The third set of serial sections shows that Al-B weakly stains in a fibroblastic focus (A), whereas the expression of type I collagen (B) and ICTP (C) is observed in the whole ECM of the focus. D, The expression of PICP is observed in fibroblasts of the focus. Hematoxylin (A-D) and Resorcin-fuchsin (B-D) for counterstain. Scale bar represents 100  $\mu$ m.

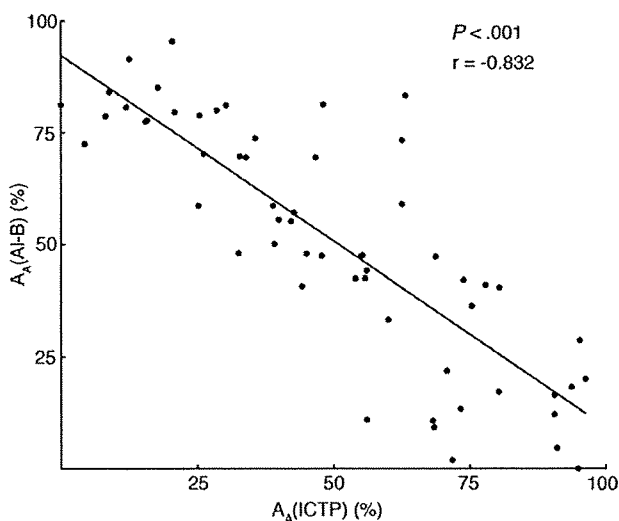


**Fig. 4** A negative correlation between Al-B<sup>+</sup> and ICTP<sup>+</sup> area densities in fibroblastic foci. Morphometric analysis demonstrates that there is a significantly inverse correlation between  $A_A(\text{Al-B})$  and  $A_A(\text{ICTP})$ .

deposition of GAGs and collagen; and stage III, characterized by collagen-dominant deposition. All 3 stages were detectable in the specimens of almost all patients, suggesting that this pathologic staging represents the fibrogenic processes occurring in FF but not the differences in the etiology and outcome of IPF.

It was noted that, in stage I, type I collagen was barely deposited in the ECM, although PICP was already expressed in the fibroblasts. Typically, procollagen is secreted from the fibroblasts and cleaved by proteases to form collagen fibrils, the basic structural units of a collagen fiber/tendon. This is followed by the cross-linking of collagen [37]. There is limited information regarding the factors regulating the release of procollagen by fibroblasts. In our study, morphological observation showed that the expression of ICTP was distributed in the lesions where GAGs were degraded. We speculate that an inhibitory factor may be actively involved in inhibiting the secretion of procollagen from fibroblasts in stage I. For example, PGs may prevent fibroblasts from releasing procollagen via integrin signals.

**Table 2** The profile of the patients with IPF

Patient	Age/sex	Total/FF (stage I/II/III) <sup>a</sup>
1	58/F	7 (1/3/3)
2	69/M	23 (10/9/4)
3	78/M	9 (2/5/2)
4	58/F	4 (0/3/1)
5	67/F	24 (5/12/7)
6	58/F	10 (6/3/1)
7	64/M	8 (2/4/2)
8	63/F	6 (1/2/3)
9	66/M	10 (1/4/5)
10	67/M	7 (0/4/3)
11	50/M	4 (2/1/1)
12	76/M	7 (5/2/0)
13	67/F	14 (5/6/4)
14	63/M	5 (1/4/0)
15	57/M	9 (3/4/1)
16	52/M	2 (0/2/0)

<sup>a</sup> The number of FF in each stage.

There has been increasing evidence in support of MMP-2 and TIMP-2 involvement in matrix turnover in cases of pulmonary fibrosis [16-23]. It has been shown that TIMP-2

is expressed in the overlying epithelium and fibroblasts of FF in IPF [16,17,22]. The coexpression of TIMP-2 and Ki-67 (a marker for cell proliferation) was observed in the fibroblasts of FF [18]. The findings of these reports suggest that TIMP-2 is involved in the stable deposition of collagen and fibronectin, as well as the regulation of fibroblast proliferation. It has been reported that MMP-2 is also expressed in the fibroblasts of FF [22]. Batimastat—a synthetic inhibitor of MMPs—mainly down-regulates MMP-2 and MMP-9 in mice with bleomycin-induced pulmonary fibrosis; moreover, the down-regulation of MMPs was associated with a decrease in the proliferation of fibroblasts. Furthermore, this down-regulation was associated with a decrease in collagen deposition [38]. In these reports, it was speculated that the inconsistent expression of MMP-2 may contribute to the degradation of the epithelial basement membrane, thus facilitating the migration of fibroblasts into the FF.

In the present study, the expression of MMP-2 and TIMP-2 in FF during stage I was observed in overlying epithelial cells and in the fibroblasts of the FF. In the later stages, however, the expression of TIMP-2 was attenuated in all cells of the FF. In contrast, the expression of MMP-2 was

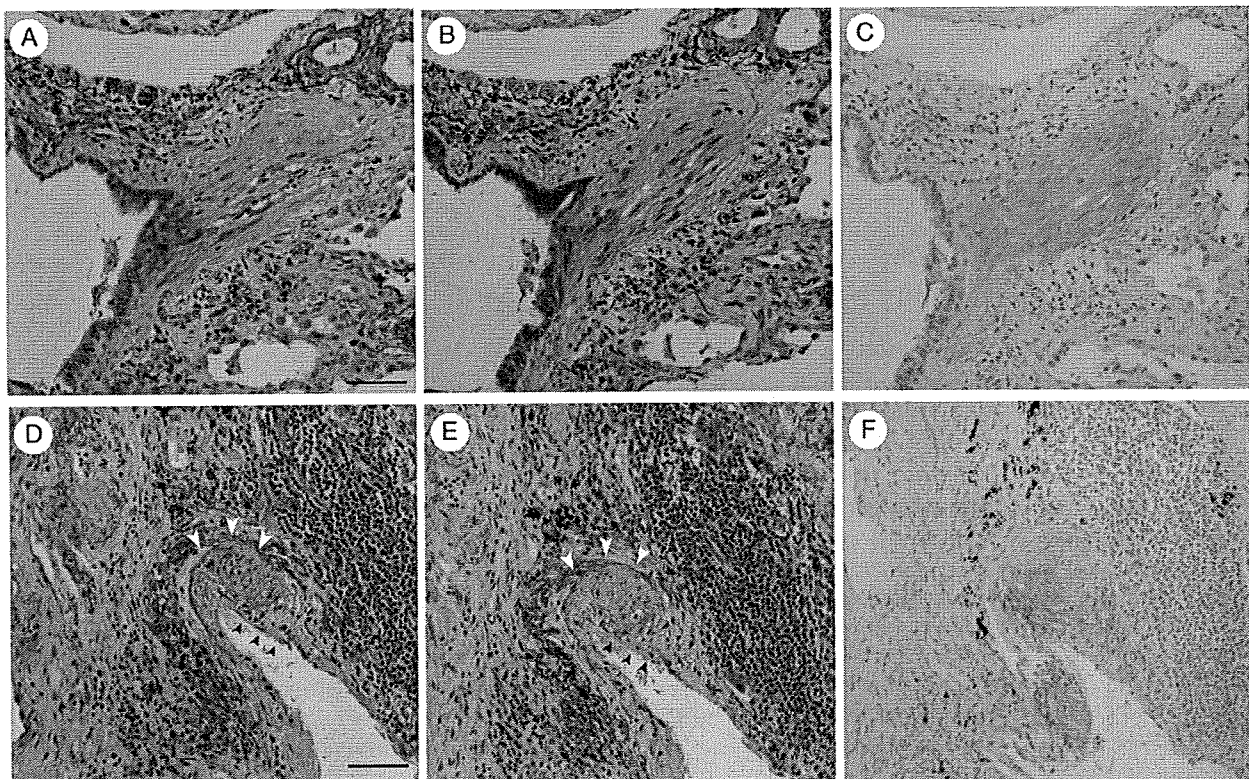


**Fig. 5** Characterization of MMP-2 and TIMP-2 expression in the 3 stages. The upper set of serial sections (A-C) shows that the expression of MMP-2 (A) and TIMP-2 (B) is observed in fibroblasts and the overlying epithelium in stage I. The lower set of serial sections (D-F) shows that the expression of MMP-2 (D) persists in fibroblasts in the later stage (white arrowheads), although it is not observed in the overlying epithelium (black arrowheads). (E) In contrast, the expression of TIMP-2 is attenuated both in fibroblasts (white arrowheads) and the overlying epithelium (black arrowheads). C and F, Al-B staining. Hematoxylin (A-F) and Resorcin-fuchsin (A, B, D, and F) for counterstain. Scale bar represents 100  $\mu$ m.

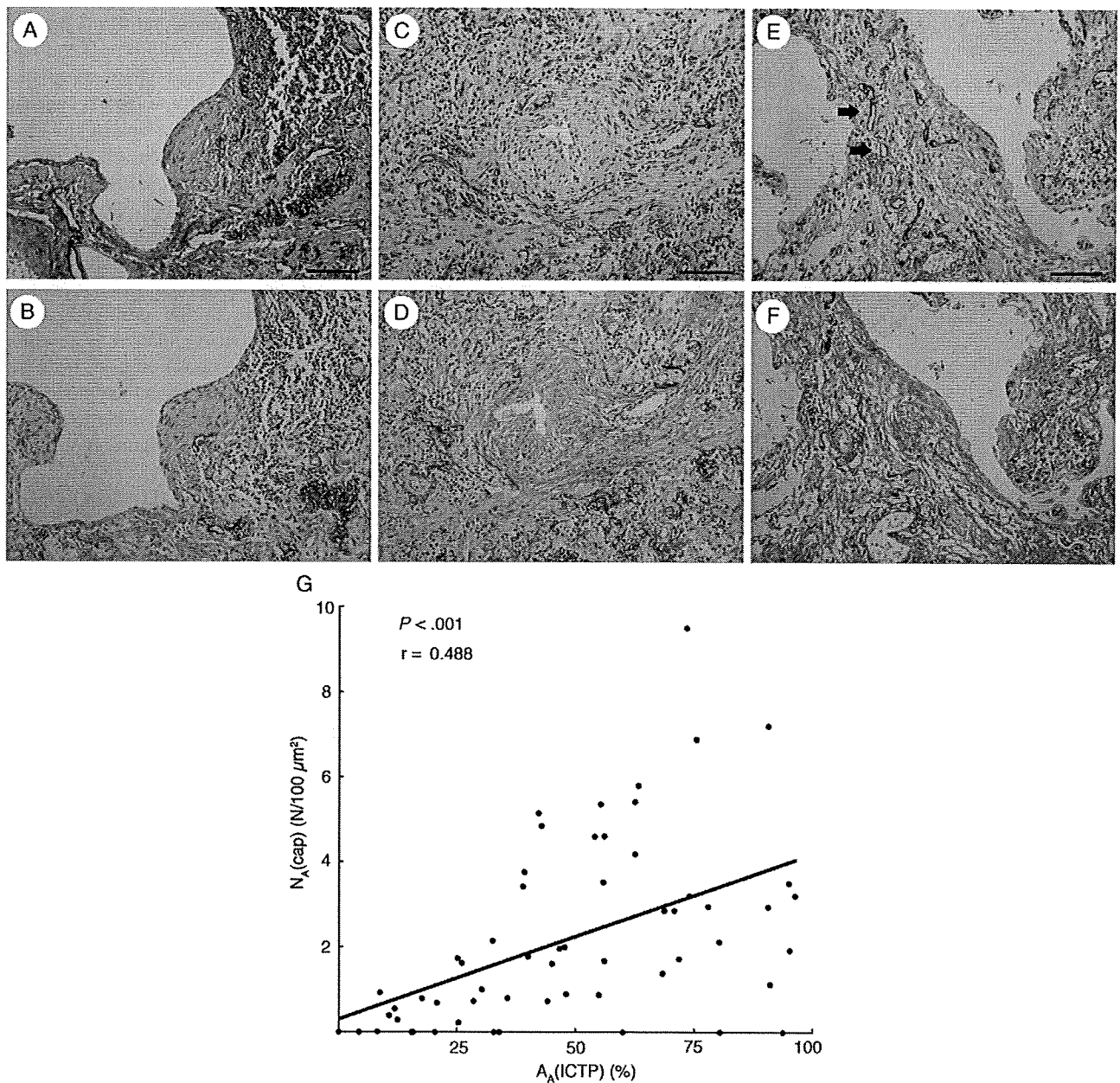


**Fig. 6** Characterization of capillary angiogenesis and lymphangiogenesis in the 3 stages. A and B, A set of serial sections shows that CD34<sup>+</sup> capillaries (red in A) are not observed in a ICTP<sup>weak</sup> fibroblastic focus (B) in stage I. C and D, Another set of serial sections shows that in stage II, several CD34<sup>+</sup> capillaries (red in C) are observed in the peripheral ICTP<sup>+</sup> lesions of a fibroblastic focus (D), although undetectable in the inner ICTP<sup>weak</sup> side. E and F, The other of serial sections shows that CD34<sup>+</sup> capillaries (red in E) are widely distributed in a ICTP<sup>+</sup> fibroblastic focus (F) in stage III. D2-40<sup>+</sup> lymphatic vessels (brown in A, C, and E) are not found in FF across all 3 stages, although they can be detected outside FF (arrows in E). (G) Morphometric analysis demonstrates that there is a significant correlation between  $A_A(\text{ICTP})$  and  $N_A(\text{cap})$ . Hematoxylin and Resorcin-Fuchsin for counterstain. Scale bar represents 100  $\mu\text{m}$ .

found to persist in the fibroblasts of the FF, where GAGs were characteristically degraded. MMP-2 has been shown to regulate the degradation of PGs [39,40]. Our results suggest that TIMP-2 contributes to the stabilization of GAG deposition in the earlier stage (stage I), whereas MMP-2 may participate in PG degradation in the later stages (stages

II and III). It was noted that apart from the overlying epithelium, the periphery of the FF also showed degradation of GAGs in stage II. These findings imply that the overlying epithelial cells strongly regulate GAG turnover.

The relationship between capillary angiogenesis and pulmonary fibrosis is interesting [24-29]. In some reports,

capillaries in FF have been shown to be barely detectable in IPF [28,29]. In contrast, Masson's body—an organized fibrotic lesion that is manifested in cryptogenic organizing pneumonia—was observed to be highly capillarized [27]. Because the fibrosis of Masson's body is dissolvable, it has been hypothesized that the absence of capillaries in FF may correlate to the poor prognosis of IPF. In the present study, the capillaries were observed in the later stages, an observation inconsistent with the previous findings. A positive correlation was observed between  $A_A$ (ICTP) and  $N_A$ (cap), and MMP-2 has been reported to induce capillary angiogenesis [41-43]. In cases of IPF, MMP-2 in fibroblasts may facilitate capillary angiogenesis in the later stages. It is still unknown whether delayed capillary formation in FF is involved in the pathogenesis of IPF.

In contrast to capillary angiogenesis, lymphangiogenesis was barely detected in FF throughout the 3 stages. Lymphangiogenesis has been reported in various pathophysiological conditions such as tumor metastasis and inflammatory conditions; however, there is limited information regarding lymphangiogenesis in the case of pulmonary fibrosis [44-46]. In wound healing, lymphangiogenesis occurs after angiogenesis through sprouting of preexisting lymphatics, and the resultant lymphatic system is transient [46]. However, in a prolonged healing process such as that associated with chronic skin ulcer, lymphangiogenesis occurs to a lesser extent than in the case of the normal healing process [46]. It has been hypothesized that newly formed lymphatics play a pivotal role in the later stages of wound healing. Pulmonary fibrosis is believed to be a consequence of aberrant healing after a lung injury [1]. It would be interesting to determine whether the absence of lymphangiogenesis in FF is associated with the indissoluble deposition of collagen in FF.

We have previously reported that, in idiopathic DAD, lymphangiogenesis was observed in the intra-alveolar fibrotic lesions during the proliferative stage, in which capillary angiogenesis was absent [31]. The intra-alveolar fibrotic lesions in DAD are similar to the FF in IPF in terms of irreversible fibroproliferation, but the results of the histopathologic characterization of the 2 types of angiogenesis in DAD were in contrast to those of the present study. The reason why capillary angiogenesis and lymphangiogenesis show contrasting features between the 2 conditions is unclear. These results indicate that the dominance of neither capillary angiogenesis nor lymphangiogenesis is related to the irreparability of pulmonary fibrosis.

In conclusion, this is the first report to demonstrate that the factors involved in tissue remodeling in IPF, including MMP-2 and TIMP-2, and the 2 types of angiogenesis show different histopathologic characteristics among the 3 stages. The findings of the present study provide new insight into the roles of these factors in tissue remodeling. The pathologic stages elucidated in this study will facilitate further investigations regarding the fibrogenic processes in IPF.

## Acknowledgments

The authors thank Dr Keiichi Saito for their excellent helps.

## References

- [1] Selman M, King TE, Pardo A, American Thoracic Society, European Respiratory Society, American College of Chest Physicians. Idiopathic pulmonary fibrosis: prevailing and evolving hypotheses about its pathogenesis and implications for therapy. *Ann Intern Med* 2001;134:136-51.
- [2] Katzenstein AL, Myers JL. Idiopathic pulmonary fibrosis: clinical relevance of pathologic classification. *Am J Respir Crit Care Med* 1998;157:1301-15.
- [3] Basset F, Ferrans VJ, Soler P, et al. Intraluminal fibrosis in interstitial lung disorders. *Am J Pathol* 1986;122:443-61.
- [4] Katzenstein AL, Myers JL, Prophet WD, et al. Bronchiolitis obliterans and usual interstitial pneumonia. A comparative clinicopathologic study. *Am J Surg Pathol* 1986;10:373-81.
- [5] Myers JL, Katzenstein AL. Epithelial necrosis and alveolar collapse in the pathogenesis of usual interstitial pneumonia. *Chest* 1988;94:1309-11.
- [6] Kuhn 3rd C, Boldt J, King Jr TE, et al. An immunohistochemical study of architectural remodeling and connective tissue synthesis in pulmonary fibrosis. *Am Rev Respir Dis* 1989;140:1693-703.
- [7] Kuhn C, McDonald JA. The roles of the myofibroblast in idiopathic pulmonary fibrosis. Ultrastructural and immunohistochemical features of sites of active extracellular matrix synthesis. *Am J Pathol* 1991;138:1257-65.
- [8] King Jr TE, Schwarz MI, Brown K, et al. Idiopathic pulmonary fibrosis: relationship between histopathologic features and mortality. *Am J Respir Crit Care Med* 2001;164:1025-32.
- [9] Nicholson AG, Fulford LG, Colby TV, et al. The relationship between individual histologic features and disease progression in idiopathic pulmonary fibrosis. *Am J Respir Crit Care Med* 2002;166:173-7.
- [10] Hanak V, Ryu JH, de Carvalho E, et al. Profusion of fibroblast foci in patients with idiopathic pulmonary fibrosis does not predict outcome. *Respir Med* 2008;102:852-6.
- [11] Selman M, Montano M, Ramos C, et al. Concentration, biosynthesis and degradation of collagen in idiopathic pulmonary fibrosis. *Thorax* 1986;41:355-9.
- [12] Lammi L, Ryhänen L, Lakari E, et al. Type III and type I procollagen markers in fibrosing alveolitis. *Am J Respir Crit Care Med* 1999;159:818-23.
- [13] Kaartecnahto-Wiik R, Lammi L, Lakari E, et al. Localization of precursor proteins and mRNA of type I and III collagens in usual interstitial pneumonia and sarcoidosis. *J Mol Histol* 2005;36:437-46.
- [14] Fukuda Y, Basset F, Ferrans VJ, et al. Significance of early intra-alveolar fibrotic lesions and integrin expression in lung biopsy specimens from patients with idiopathic pulmonary fibrosis. *HUM PATHOL* 1995;26:53-61.
- [15] Motomiya M, Arai H, Sato H, et al. Increase of dermatan sulfate in a case of pulmonary fibrosis. *Tohoku J Exp Med* 1975;115:361-5.
- [16] Hayashi T, Stetler-Stevenson WG, Fleming MV, et al. Immunohistochemical study of metalloproteinases and their tissue inhibitors in the lungs of patients with diffuse alveolar damage and idiopathic pulmonary fibrosis. *Am J Pathol* 1996;149:1241-56.
- [17] Fukuda Y, Ishizaki M, Kudoh S, et al. Localization of matrix metalloproteinases-1, -2, and -9 and tissue inhibitor of metalloproteinase-2 in interstitial lung diseases. *Lab Invest* 1998;78:687-98.
- [18] Selman M, Ruiz V, Cabrera S, et al. TIMP-1, -2, -3, and -4 in idiopathic pulmonary fibrosis. A prevailing nondegradative lung microenvironment? *Am J Physiol Lung Cell Mol Physiol* 2000;279:L562-74.

- [19] Suga M, Iyonaga K, Okamoto T, et al. Characteristic elevation of matrix metalloproteinase activity in idiopathic interstitial pneumonias. *Am J Respir Crit Care Med* 2000;162:1949-56.
- [20] Lemjabbar H, Gosset P, Lechapt-Zalcman E, et al. Overexpression of alveolar macrophage gelatinase B (MMP-9) in patients with idiopathic pulmonary fibrosis: effects of steroid and immunosuppressive treatment. *Am J Respir Cell Mol Biol* 1999;20:903-13.
- [21] Ramos C, Montaña M, García-Alvarez J, et al. Fibroblasts from idiopathic pulmonary fibrosis and normal lungs differ in growth rate, apoptosis, and tissue inhibitor of metalloproteinases expression. *Am J Respir Cell Mol Biol* 2001;24:591-8.
- [22] Kelly MM, Leigh R, Gilpin SE, et al. Cell-specific gene expression in patients with usual interstitial pneumonia. *Am J Respir Crit Care Med* 2006;174:557-65.
- [23] Oggioni T, Morbini P, Inghilleri S, et al. Time course of matrix metalloproteinases and tissue inhibitors in bleomycin-induced pulmonary fibrosis. *Eur J Histochem* 2006;50:317-25.
- [24] Keane MP, Arenberg DA, Lynch III JP, et al. The CXC chemokines, IL-8 and IP-10, regulate angiogenic activity in idiopathic pulmonary fibrosis. *J Immunol* 1997;159:1437-43.
- [25] Keane MP, Belperio JA, Burdick MD, et al. ENA-78 is an important angiogenic factor in idiopathic pulmonary fibrosis. *Am J Respir Crit Care Med* 2001;164:2239-42.
- [26] Lappi-Blanco E, Soini Y, Kinnula V, et al. VEGF and bFGF are highly expressed in intraluminal fibromyxoid lesions in bronchiolitis obliterans organizing pneumonia. *J Pathol* 2002;196:220-7.
- [27] Lappi-Blanco E, Kaarteenaho-Wiik R, Soini Y, et al. Intraluminal fibromyxoid lesions in bronchiolitis obliterans organizing pneumonia are highly capillarized. *HUM PATHOL* 1999;30:1192-6.
- [28] Renzoni EA, Walsh DA, Salmon M, et al. Interstitial vascularity in fibrosing alveolitis. *Am J Respir Crit Care Med* 2003;167:438-43.
- [29] Cosgrove GP, Brown KK, Schiemann WP, et al. Pigment epithelium-derived factor in idiopathic pulmonary fibrosis: a role in aberrant angiogenesis. *Am J Respir Crit Care Med* 2004;170:242-51.
- [30] Bensadoun ES, Burke AK, Hogg JC, et al. Proteoglycan deposition in pulmonary fibrosis. *Am J Respir Crit Care Med* 1996;154:1819-28.
- [31] Yamashita M, Iwama N, Date F, et al. Characterization of lymphangiogenesis in various stages of idiopathic diffuse alveolar damage. *HUM PATHOL* 2009 [Electronic publication ahead of print].
- [32] Matsui K, Nagy-Bojarsky K, Laakkonen P, et al. Lymphatic microvessels in the rat remnant kidney model of renal fibrosis: aminopeptidase p and podoplanin are discriminatory markers for endothelial cells of blood and lymphatic vessels. *J Am Soc Nephrol* 2003;14:1981-9.
- [33] Ishikawa Y, Akishima-Fukasawa Y, Ito K, et al. Lymphangiogenesis in myocardial remodeling after infarction. *Histopathology* 2007;51:345-53.
- [34] American Thoracic Society. Idiopathic pulmonary fibrosis: diagnosis and treatment. International consensus statement. American Thoracic Society (ATS), and the European Respiratory Society (ERS). *Am J Respir Crit Care Med* 2000;161:646-64.
- [35] Risteli J, Elomaa I, Niemi S, et al. Radioimmunoassay for the pyridinoline cross-linked carboxy-terminal telopeptide of type I collagen: a new serum marker of bone collagen degradation. *Clin Chem* 1993;39:635-40.
- [36] Weibel ER. Stereological methods. Volume 1. Practical methods for biological morphometry. Orlando (Fla): Academic Press; 1979. p. 26-39.
- [37] Kumar V, Abbas AK, Fausto N. Robbins and Cotran. Pathologic basis of disease. 7th ed. Philadelphia, Pennsylvania: Elsevier Saunders; 2005. p. 103-6.
- [38] Corbel M, Caulet-Maugendre S, Germain N, et al. Inhibition of bleomycin-induced pulmonary fibrosis in mice by the matrix metalloproteinase inhibitor batimastat. *J Pathol* 2001;193:538-45.
- [39] Zuo J, Ferguson TA, Hernandez YJ, et al. Neuronal matrix metalloproteinase-2 degrades and inactivates a neurite-inhibiting chondroitin sulfate proteoglycan. *J Neurosci* 1998;18:5203-11.
- [40] Passi A, Negrini D, Albertini R, et al. The sensitivity of versican from rabbit lung to gelatinase A (MMP-2) and B (MMP-9) and its involvement in the development of hydraulic lung edema. *FEBS Lett* 1999;456:93-6.
- [41] Rivilis I, Milkiewicz M, Boyd P, et al. Differential involvement of MMP-2 and VEGF during muscle stretch- versus shear stress-induced angiogenesis. *Am J Physiol Heart Circ Physiol* 2002;283:H1430-8.
- [42] Ohno-Matsui K, Uetama T, Yoshida T, et al. Reduced retinal angiogenesis in MMP-2-deficient mice. *Invest Ophthalmol Vis Sci* 2003;44:5370-5.
- [43] Zheng H, Takahashi H, Murai Y, et al. Expressions of MMP-2, MMP-9 and VEGF are closely linked to growth, invasion, metastasis and angiogenesis of gastric carcinoma. *Anticancer Res* 2006;26:3579-83.
- [44] Skobe M, Hawighorst T, Jackson DG, et al. Induction of tumor lymphangiogenesis by VEGF-C promotes breast cancer metastasis. *Nat Med* 2001;7:192-8.
- [45] Baluk P, Tammela T, Ator E, et al. Pathogenesis of persistent lymphatic vessel hyperplasia in chronic airway inflammation. *J Clin Invest* 2005;115:247-57.
- [46] Paavonen K, Puolakkainen P, Jussila L, et al. Vascular endothelial growth factor receptor-3 in lymphangiogenesis in wound healing. *Am J Pathol* 2000;156:1499-504.



